

# On the dynamics of a deep quasi-permanent anticyclonic eddy in the Rockall Trough

M. Le Corre<sup>\*,a</sup>, J. Gula<sup>a</sup>, A. Smilenova<sup>b,c</sup>, L. Houpert<sup>d</sup>

a. Laboratoire d'Océanographie Physique et Spatiale (LOPS), Université de Bretagne Occidentale (UBO), Institut Universitaire Européen de la Mer (IUEM)

b. Earth and Ocean Sciences, School of Natural Sciences, National University of Ireland, Galway (NUIG), University Road, Galway, Ireland, H91 TK33

c. Oceanographic Services, Ocean Sciences and Information Services (OSIS), Rinvillle, Co. Galway, Marine Institute, Ireland, H91 R673

d. National Oceanography Centre (NOC), European Way, Marine Physics and Ocean Climate Division, Southampton, England, UK, SO14 3ZH

\* . Corresponding author at : LOPS, UBO, IUEM. E-mail address : mathieu.lecorre@univ-brest.fr(M. Le Corre)

## Résumé :

*Une étude récente a montré l'existence d'un anticyclone profond quasi-permanent dans le Rockall Trough (RT) à l'ouest de l'Irlande. Ce tourbillon est localisé au croisement de différentes masses d'eau qui interagissent entre elles. Nous nous intéressons ici à la création et l'évolution de cet anticyclone à l'aide de simulations numériques à haute-résolution avec le modèle océanique CROCO. Nous montrons que la source principale de vorticité anticyclonique est la divergence des flux de vorticité tourbillonnaires, ceux-ci étant équilibrés par des effets de topographie et de frottements au fond. Ce flux de vorticité tourbillonnaire est majoritairement associé à l'advection de vorticité par des anticyclones de plus petite échelle, formés le long du bord est du RT. L'interaction entre le courant méridional, qui s'écoule vers le nord le long du Porcupine Bank, et la topographie permet de générer de la vorticité négative dans la couche limite de fond. Le détachement de cette vorticité à différents emplacements produit de l'instabilité centrifuge et conduit à la formation de tourbillon de méso et sous-mésoéchelle. Ces tourbillons sont ensuite transportés vers le centre du RT et fusionnent avec l'anticyclone, l'alimentant ainsi en permanence avec de la vorticité anticyclonique.*

## Abstract :

*A recent study has put into perspective the presence of a quasi-permanent deep anticyclonic eddy in the Rockall Trough (RT), west of Ireland. This eddy is located at a crossroad where different water masses meet and interact with each other. Using a truly mesoscale resolving simulation with a terrain following coordinate ocean model (CROCO), we study the generation and life-cycle of the RT anticyclone. We show that the main source of anticyclonic vorticity for the RT anticyclone is the divergence of eddy vorticity fluxes. Eddy vorticity fluxes are mostly due to the advection of vorticity by anticyclonic submesoscale coherent vortices generated on the eastern RT slope. Interactions between the current flowing poleward*

*along the Porcupine Bank, on the eastern side of the RT, and the slope induce anticyclonic vorticity generation in the bottom boundary layer. Detachment of the vorticity layer from the slope at specific locations induces centrifugal instability and formation of anticyclonic eddies. These eddies are then advected toward the center of the RT and merge with the RT anticyclone, continuously feeding it with anticyclonic vorticity.*

## Mots clefs : Regional Oceanic Modelling System ; eddy ; interaction current topography ; vorticity

### 1 Introduction

The subpolar North Atlantic gyre is a key region for the ocean heat and carbon budgets. Mesoscale eddies, with a radius in the range 10-100 km, play a big role in modulating the heat and carbon fluxes [1]. The distribution of eddy kinetic energy (EKE) computed from Argo floats at depth (1000–1500-m) in the subpolar North Atlantic gyre highlights the presence of energetic mesoscale eddies in the different basins [2]. Hot spots are visible in the Labrador Sea, where Irminger Rings are regularly shedded due to instabilities of the Irminger current, and in the Iceland Basin and Rockall Trough (RT), where supoplar waters enter through the North Atlantic Current [3].

A strong EKE signal associated with a mean anticyclonic circulation is visible at depth in the RT at 12° W, 55° N from the Argo floats database [2]. A surface signature has also been spotted at the same location from altimetry [4]. In-situ observations have recently highlighted that this signal was linked to the presence of a quasi-permanent deep anticyclonic vortex : the RT anticyclone [5].

The signature of the RT anticyclone is also clearly visible in the Eddy Available Potential Energy (EAPE, figure 1a). The EAPE represents the amount of energy stored in the vertical isopycnal displacements and is a signature of the mesoscale turbulence [6]. The strong signal in the RT highlights the recurrent presence of the eddy, generating large vertical isopycnal displacements at around 1000-m.

Similar deep quasi-permanent eddies can be found in other parts of the ocean. One well studied example is the Lofoten Vortex [12, 13]. Dynamical studies of this feature have put forward the importance of smaller scale eddies for its formation and variability [14].

Numerical models with horizontal resolutions up to 1/12° do not seem able to reproduce the RT anticyclone [11]. Thus, we hypothesize that scales smaller than the local Rossby deformation radius ( $Rd \approx 10 - 20$  km) may be important for the generation and dynamics of the RT anticyclone. This highlights the need for a truly mesoscale-resolving model in this area.

In this study we investigate the dynamics of the RT anticyclone using a high resolution simulation ( $dx = 2$  km). The paper is organized as follows : The numerical model is presented and validated in Section 2. A barotropic vorticity balance for the RT anticyclone is analyzed in section 3. In section 4 we investigate the generation of small scale eddies close to the topography. Finally in section 5 we track the origin of the different water masses using a Lagrangian approach.

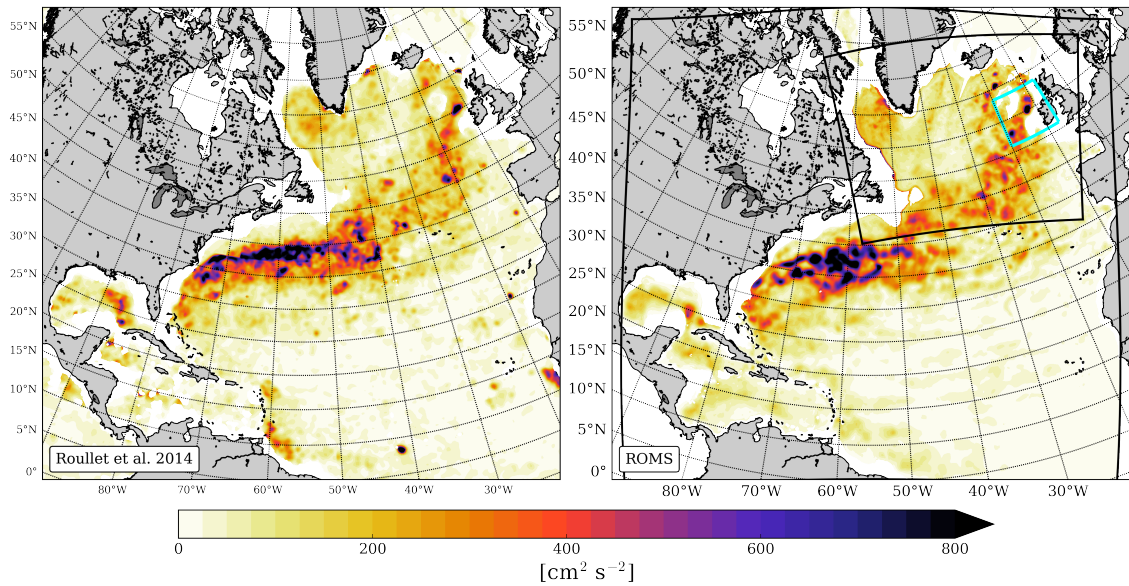


FIGURE 1 – Eady Available Potential Energy (EAPE) at 1000-m computed from Argo data (left) and from the CROCO simulations (right). The black contours represent the nested domains and the cyan contour the area of study.

## 2 Model setup

To study the dynamics of the RT vortex, we use a terrain-following coordinate model : the Regional Oceanic Modelling System (ROMS, [15]) in its CROCO (Coastal and Regional Ocean Community) version [16]. It solves the hydrostatic primitive equation for velocity, temperature, and salinity, using a full equation of state for seawater [15].

We use a one way nesting approach by defining two successive horizontal grids with resolutions  $\Delta x \approx 6$  km for the parent grid covering the North Atlantic ocean and  $\Delta x \approx 2$  km for the child grid covering the subpolar gyre. It allows the simulation to be truly eddy resolving in most of the area, as the Rossby deformation radius varies between 10 and 20 km over the region [17]. The domains are shown in Figure 1 along with the area of interest highlighted in cyan.

The North Atlantic and subpolar gyre simulations have 50 and 80 vertical levels, respectively. Vertical levels are stretched at the surface and bottom [18] to have a better representation of the surface layer dynamics at the top and flow-topography interactions at the bottom. The vertical mixing of tracers and momentum is done by a  $k-\epsilon$  model (GLS, [19]). The effect of bottom friction is parameterized through a logarithmic law of the wall with a roughness length  $Z_0 = 0.01$  m.

The representation of the mesoscale activity in our simulations can be evaluated through the EAPE at 1000-m (figure 1). The modelled EAPE matches well with the EAPE evaluated using Argo data [6]. We retrieve the high amplitude associated with the Gulf Stream and the North Atlantic Current. In the RT, both model and observations show a local maximum with comparable amplitude northwest of Ireland, related to the presence of the RT anticyclone.

The mean vertical structure of the flow at this location is shown in Figure 2,b for the model along with in-situ observations from Smilanova et al, 2019 [5]. Observations shown in Figure 2,a correspond to a transect done in January 2011. The observational velocity is derived from the temperature and salinity measurements assuming geostrophic balance.

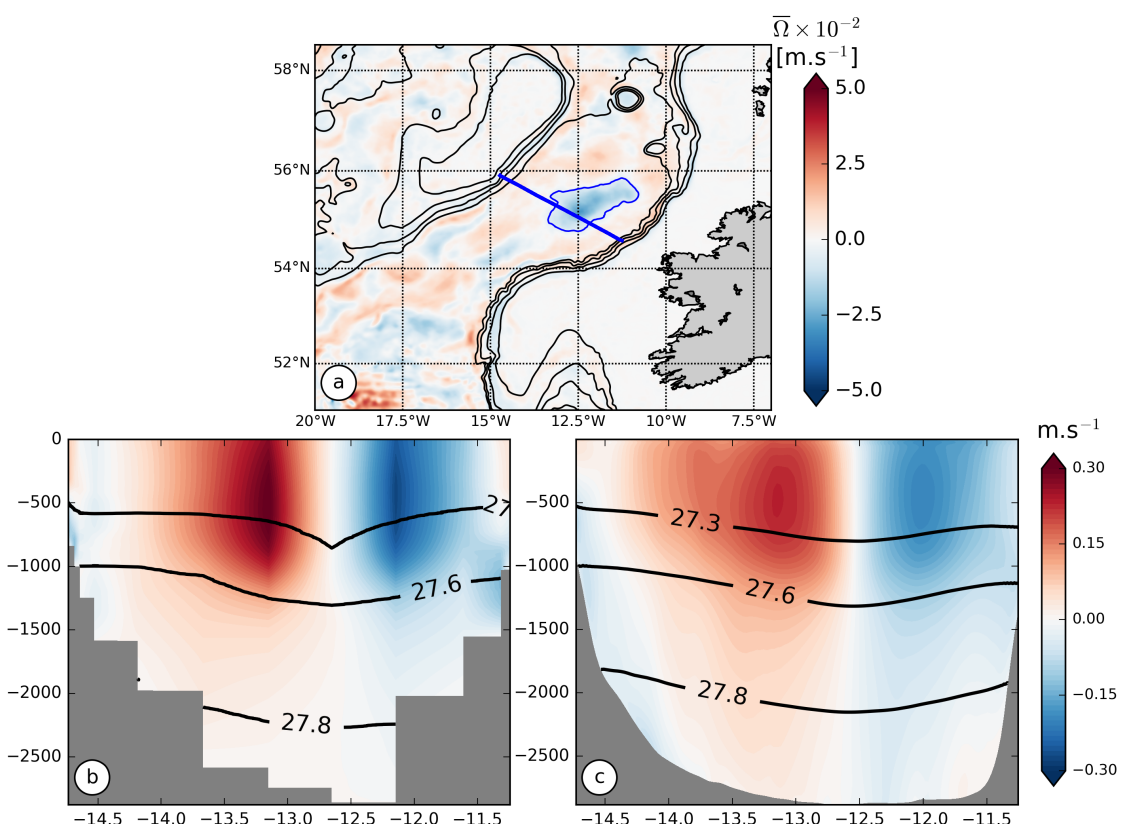


FIGURE 2 – (a) One-year mean of barotropic vorticity from the model. (b-c) Vertical sections of potential density (black contours) and cross-section velocity (colors) along the section shown in blue in panel a from in-situ observations in January 2011 (a) and from the model (b).

### 3 On the dynamics of the Rockall Trough anticyclone

#### 3.1 Barotropic vorticity balance

The RT anticyclone has a strong barotropic signature (Fig. 2). An effective way to understand its dynamics is to look at the balance of barotropic vorticity. Such balance will provide information on the sources and sinks of anticyclonic vorticity and help us understand how the circulation can be sustained over such a long period.

The barotropic vorticity is defined as the vorticity of the vertically integrated velocities [20] :

$$\Omega = \frac{\partial \bar{v}}{\partial x} - \frac{\partial \bar{u}}{\partial y}$$

with  $(u, v)$  the  $(x, y)$  components of the horizontal flow, and the overbar denotes a vertically integrated quantity,

$$\bar{u} = \int_{-h}^{\zeta} u \, dz,$$

where  $\zeta(x, y, t)$  is the free-surface height and  $h(x, y) > 0$  the depth of the resting topography.  $H(i, j, t) = \int_{-h}^{\zeta} dz = \zeta(i, j, t) + h(i, j)$  is the total depth of the water column.

The evolution equation for the barotropic vorticity is obtained by integrating the momentum equations in the vertical and cross differentiating them :

$$\underbrace{\frac{\partial \Omega}{\partial t}}_{\text{rate}} = - \underbrace{\nabla \cdot (f \bar{u})}_{\text{planet. vort. adv.}} + \underbrace{\frac{J(P_b, h)}{\rho_0}}_{\text{bot. pres. torque}} + \underbrace{k \cdot \nabla \times \frac{\tau_{wind}}{\rho_0}}_{\text{wind curl}} - \underbrace{k \cdot \nabla \times \frac{\tau_{bot}}{\rho_0}}_{\text{bot. drag curl}} + \underbrace{D_{\Sigma}}_{\text{horiz. diffusion}} - \underbrace{A_{\Sigma}}_{\text{NL advection}}$$

Integrated over a long enough period, the rate becomes negligible compared to the other terms, and the time-mean planetary vorticity advection reduces to  $\langle -\nabla \cdot (f \bar{u}) \rangle = \langle -\beta \bar{V} - f \frac{\partial \eta}{\partial t} \rangle \approx \langle -\beta \bar{V} \rangle$  as  $\langle \frac{\partial \eta}{\partial t} \rangle \approx 0$ , where brackets corresponds to a time mean,  $\beta = df/dy$  is the variation of the Coriolis parameter with latitude and  $V$  the velocity in the latitudinal direction. After one year of integration, the amplitude of the rate is already at least one order of magnitude smaller than the other terms.

The Bottom Pressure Torque (BPT) arises from the variation of bottom pressure along isobaths. It represents the contribution of the topography to the barotropic vorticity balance. This term is essential in balancing the zonal wind stress curl for subpolar gyres and in locally balancing the planetary vorticity advection for Western Boundary Current systems [21].

The non-linear term (NL) encompasses all non-linearities. It can be written as :

$$A_{\Sigma} = \frac{\partial^2 (\bar{v}\bar{v} - \bar{u}\bar{u})}{\partial x \partial y} + \frac{\partial^2 \bar{u}\bar{v}}{\partial x \partial x} - \frac{\partial^2 \bar{u}\bar{v}}{\partial y \partial y}$$

The viscosity effects are included in the  $D_{\Sigma}$  term and the stress curls at the bottom and surface are respectively  $\nabla \times \frac{\tau_{bot}}{\rho_0}$  and  $\nabla \times \frac{\tau_{wind}}{\rho_0}$ .

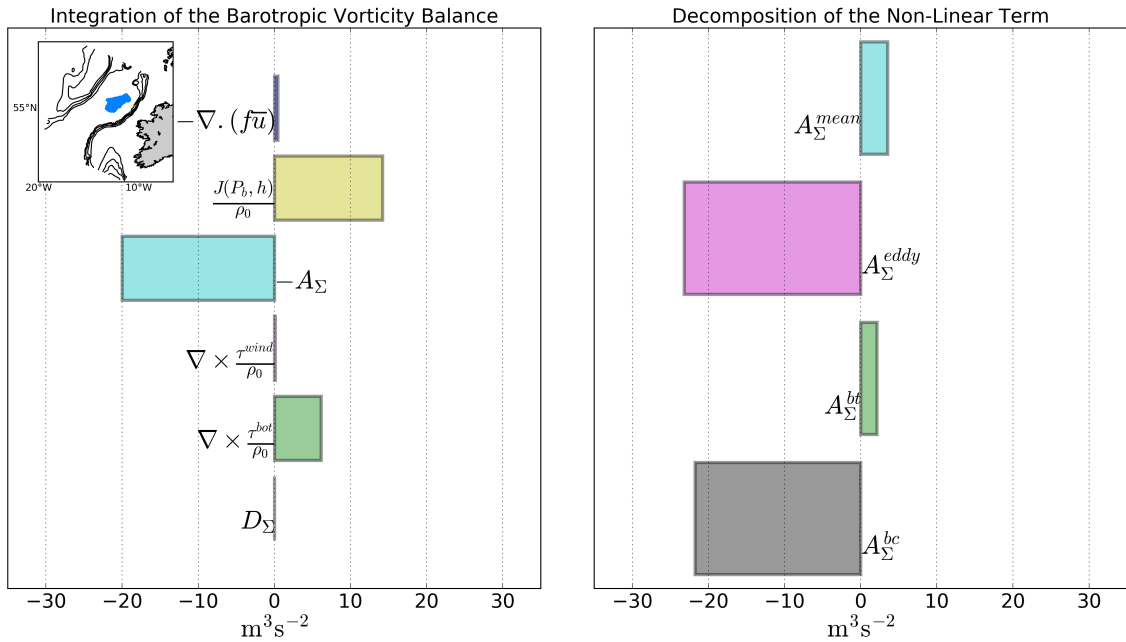


FIGURE 3 – Integration of the Barotropic Vorticity balance over the RT anticyclone (left) and decompositions of the non-linear term between mean and eddy components, and between barotropic and baroclinic components (right)

The different terms of the barotropic vorticity balance are integrated over an area corresponding to the mean position of the vortex (Fig 3), defined as the  $-0.005 \text{ m.s}^{-1}$  barotropic velocity amplitude contour (Fig 1). The main source for the anticyclonic circulation of the vortex is the non-linear term  $A_\Sigma$ . The main sinks of barotropic vorticity are the BPT and the Bottom Drag Curl (BDC). As a result of the small area covered by the eddy, the wind contribution is small, meaning that the wind stress does not contribute much to the vortex forcing.

### 3.2 Non-linear forcing of the RT anticyclone

The non-linear term includes both time and vertical averages of non-linear quantities. To better understand what is hidden inside, it is possible to further decompose it in a mean and an eddy part, and in a barotropic and a baroclinic part. Both decompositions are possible by writing the velocities as follows :

$$u = \langle u \rangle + u^*$$

$$u = \bar{u} + u'$$

Where  $\langle \bullet \rangle$  and  $\bar{\bullet}$  represents respectively the mean and barotropic part of the flow. The  $\bullet^*$  and  $\bullet'$  are the deviations from these averages and stand for the eddy and baroclinic part, respectively. With this decomposition of the velocity, the NL term can be written as :

$$A_\Sigma(u, v) = \underbrace{A_\Sigma(\langle u \rangle, \langle v \rangle)}_{A_\Sigma^{mean}} + \underbrace{A_\Sigma(u^*, v^*)}_{A_\Sigma^{eddy}} + \varepsilon$$

and

$$A_{\Sigma}(u, v) = \underbrace{A(\bar{u}, \bar{v})}_{A_{\Sigma}^{bt}} + \underbrace{A(u', v')}_{A_{\Sigma}^{be}}$$

,

where  $\varepsilon$  is the residue of the cross product and is negligible compared to both the mean and the eddy parts (not shown). Spatial integrations of these terms on the mean RT anticyclone area are shown in Figure 3.

The NL term is strongly dominated by its eddying part. The time-mean flow does not feed the RT anticyclone, and the vorticity is provided only by eddy vorticity fluxes. The decomposition into a barotropic and a baroclinic part also shows only one term being dominant : the baroclinic component is much larger than the barotropic one. The main source of negative barotropic vorticity for the vortex is due to baroclinic eddy vorticity fluxes.

This vorticity balance can be interpreted as the RT vortex being fed by smaller subsurface anticyclonic eddies with a localized structure in the vertical. This is illustrated by a typical example of a smaller scale anticyclonic vortex merging with the RT anticyclone (Fig. 4). Snapshots of relative vorticity at 1000-m depth show the formation of a negative vorticity filament along the Porcupine bank (figure. 4,a). The filament rolls up and form an anticyclonic eddy (figure. 4,b), which is attracted by the RT anticyclone (figure. 4,c), and is stretched around the RT anticyclone until they fully merge (figure. 4,d).

## 4 Eddy generation

The RT anticyclone seems to be fed mostly by small baroclinic anticyclonic eddies. In this section, we investigate the generation mechanisms for these smaller scale eddies.

Generation of anticyclonic eddies at this depth is mostly a result of current-topography interactions around the RT. Wintertime convection does not penetrate as deep.

The mean current is flowing cyclonically around the RT, i.e. with the shallower topography on his right. Frictional effects at the bottom will then trigger generation of negative relative vorticity and negative potential vorticity (PV) in the bottom boundary layer. When the boundary layer detaches from the slope, it can lead to centrifugal instability and formation of coherent vortices [22, 23].

The PV is defined by  $q = \omega_a \cdot \nabla b$ , with  $\omega_a = f\mathbf{z} + \nabla \times \mathbf{u}$  the absolute vorticity and the buoyancy gradient  $b = -g \frac{\sigma}{\rho_0}$  where  $\sigma$  is the potential density referenced to the surface,  $\rho_0$  the mean reference density and  $g$  the gravitational acceleration. The flux form of the PV equation can be written [24] :

$$\frac{\partial q}{\partial t} + \nabla \cdot [\underbrace{q\mathbf{u}}_{J_A} - \underbrace{\omega_a \frac{Db}{Dt}}_{J_D} + \underbrace{\nabla b \times \mathbf{F}}_{J_F}] = 0$$

where  $\mathbf{F}$  corresponds to the non conservative forces per unit mass. Each term respectively represent the PV advection, the diabatic flux and the frictional flux. When integrated between two isopycnal levels that intersect the seafloor but do not outcrop (hereafter I) the previous equation can be reduced to :

$$\frac{\partial}{\partial t} \int_I q dV = \int_I \underbrace{J_b}_{-(J_D + J_F)} dV$$

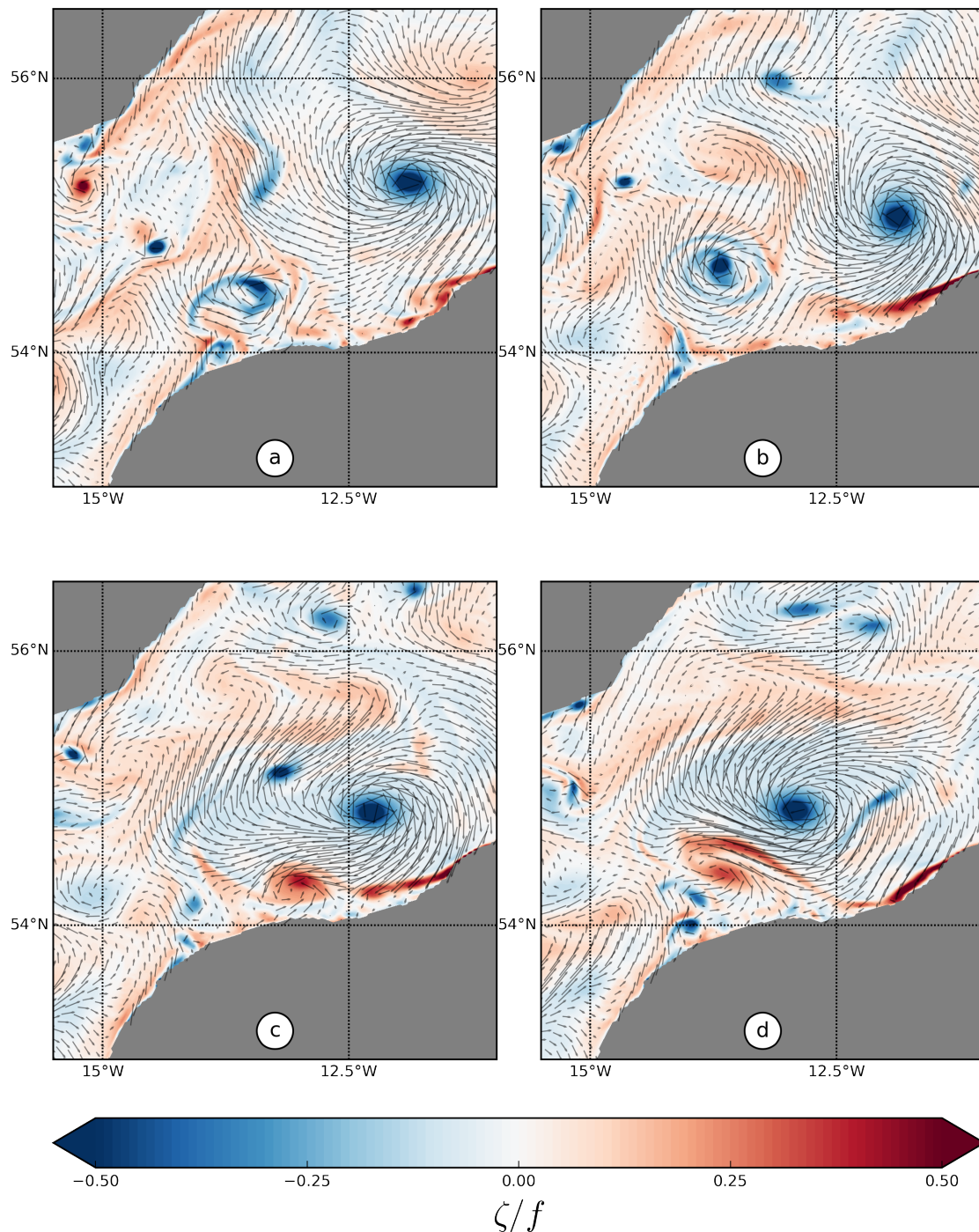


FIGURE 4 – Sequence of snapshots of  $\zeta/f$  at 1000-m depth showing the formation of a smaller eddy at Porcupine Bank later merging with the RT anticyclone. Frames are 6 days apart starting at the upper-left panel and proceed according to the labels

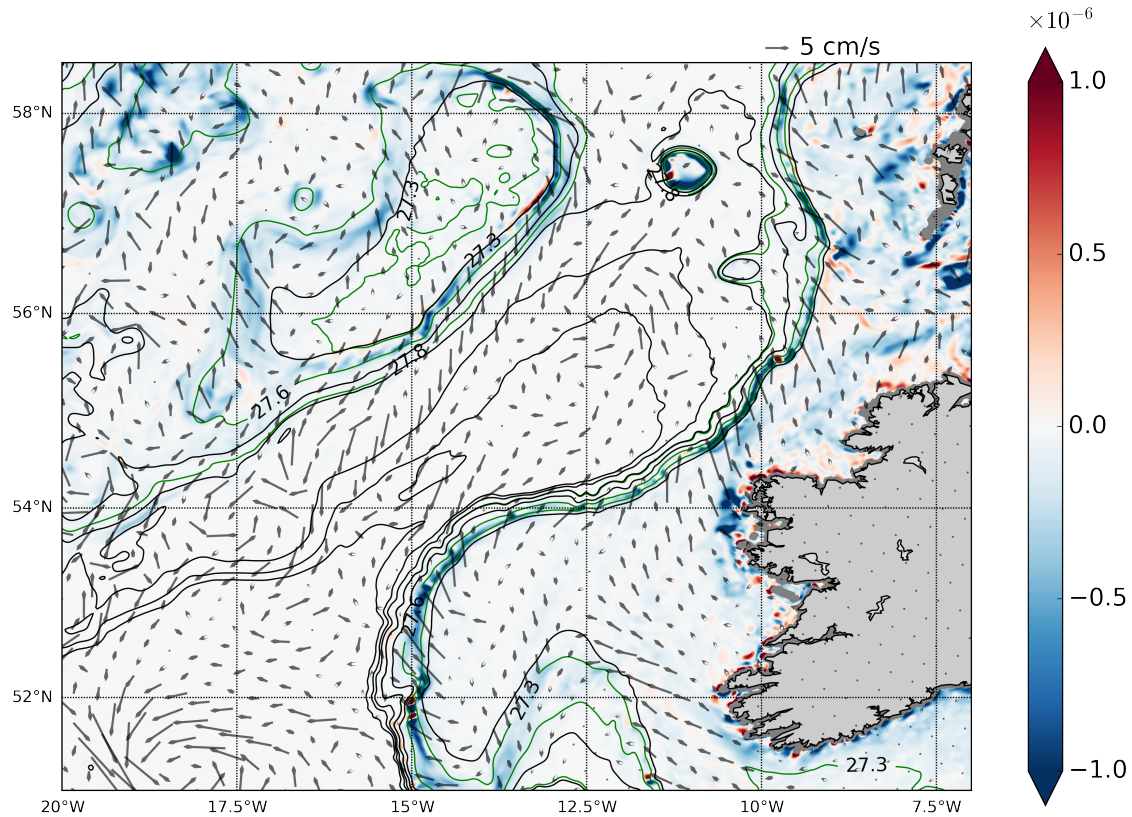


FIGURE 5 – Time mean PV flux at the bottom. The green contours correspond to the mean intersection of the  $27.3, 27.6$  and  $27.8 \text{ kg.m}^{-3}$  with the topography

,

meaning that the sources of potential vorticity along a slope are driven by diabatic and frictionnal effects. Thus, large values of the  $J_b$  vector would indicate the most likely spots for a recurrent generation of eddies.

The bottom PV fluxes are negative all around the RT (Fig. 5), in agreement with the orientation of the mean current flowing cyclonically around the RT. Hot spots are visible along the Porcupine bank and the Rockall Plateau. The strongest signals are located, on average, between the  $27.3$  and  $27.6 \text{ kg.m}^{-3}$  isopycnals. The negative PV flux is dominated by frictional fluxes, the diabatic flux tends to generate positive input of PV (not shown).

As the PV is conserved between two isopycnals, an eddy generated in a given density range will stay in this density range and move isopycnally inside the basin. Looking at the vertical structure of the vortex (Fig. 2), we see that eddies generated along the topography between the  $27.3$  and  $27.6 \text{ kg.m}^{-3}$ , on average between  $500$  and  $1000$  m, will deepen when approaching the vortex and merge with it at the base of its core.

## 5 Lagrangian tracking of water masses

We have identified the locations where anticyclonic vorticity is generated in the RT. To further investigate if the eddies generated along the slope can reach the RT anticyclone, we use a Lagrangian approach.

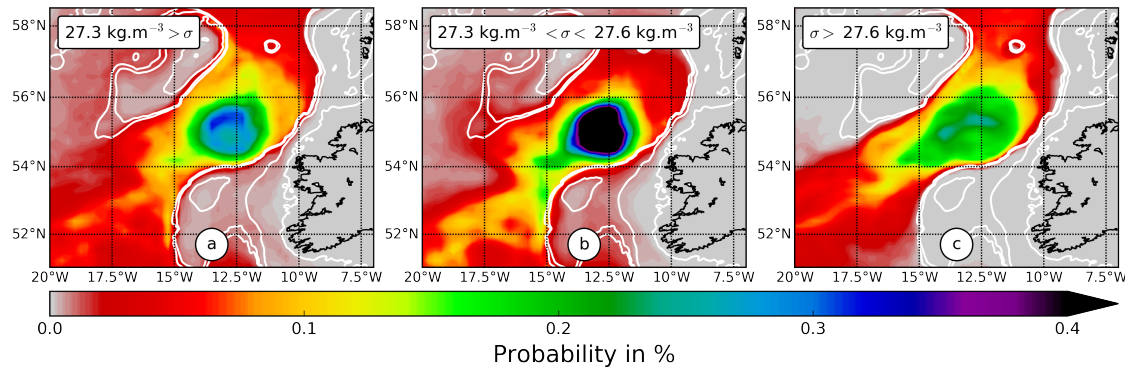


FIGURE 6 – Probability that a particle occupies a particular bin at least once during the considered time span in different density ranges

We seed neutrally buoyant Lagrangian particles at the last time step of the simulation and advect them backward in time for one year. This allows us to track their trajectories and identify where particles are coming from. The vortex is separated in three density ranges : light (lighter than  $27.3 \text{ kg.m}^{-3}$ ), intermediate (between  $27.3$  and  $27.6 \text{ kg.m}^{-3}$ ) and heavy (higher than  $27.6 \text{ kg.m}^{-3}$ ) waters. We compute the 2-D Probability Density Function (PDF) for the particles originating from each layer (Fig 6). The PDF is binned on a  $1/5^\circ$  grid and corresponds, for each bin, to the probability that a particle has been located inside this bin at least once during its lifetime [25].

Water lighter than  $27.6 \text{ kg.m}^{-3}$  is mostly originating from the current flowing northward along the Porcupine Bank, where we observe a strong anticyclonic eddy generation.

## 6 Summary and conclusion

The dynamics of a deep, quasi-permanent, non-stationary anticyclone in the Rockall Trough has been studied in a succession of nested simulations ( $\Delta x = 6$  to  $2 \text{ km}$ ) using the oceanic model CROCO.

The main source of negative vorticity for the vortex is due to eddy vorticity fluxes, mostly due to the merging of smaller anticyclonic eddies generated between 500 and 1000 m depth. This input of anticyclonic vorticity is balanced by topographic effects through the bottom pressure torque and the bottom drag curl acting as anticyclonic vorticity sinks. The intensification of the RT anticyclone implies a barotropization of its structure, which results in an intensification of the bottom currents. These currents are responsible for a positive drag curl and positive bottom pressure torque counter-acting the intensification of the RT vortex.

Thanks to a combined study using the potential vorticity flux and a Lagrangian approach we were able to locate the main generation area for these eddies along the Porcupine bank. They are created predominantly between the  $27.3$  and  $27.6 \text{ kg.m}^{-3}$  isopycnals and are reaching the RT anticyclone just below its core.

## Références

- [1] J. Zhao, A. Bower, J. Yang, X. Lin, Meridional heat transport variability induced by mesoscale processes in the subpolar North Atlantic, *Nature Communications*, 9 (2018) 1124.
- [2] J. Fischer, J. Karstensen, M. Oltmanns, S. Schmidtko, Mean circulation and EKE distribution in the Labrador Sea Water level of the subpolar North Atlantic, *Ocean Science*, 14 (2018) 1167–1183.
- [3] L. Houpert, M.E. Inall, E. Dumont, S. Gary, C. Johnson, M. Porter, W.E. Johns, S.A. Cunningham, Structure and transport of the north atlantic current in the Eastern Subpolar Gyre from sustained glider observations, *Journal of Geophysical Research : Oceans*, 123 (2018) 6019–6038.
- [4] D.L. Volkov, Interannual Variability of the Altimetry-Derived Eddy Field and Surface Circulation in the Extratropical North Atlantic Ocean in 1993–2001, *Journal of Physical Oceanography* 35 (2005) 405–426.
- [5] A. Smilenova, J. Gula, M. Le Corre, L. Houpert, On the vertical structure and generation mechanism of a deep anticyclonic vortex in the central Rockall Trough, northeast North Atlantic, To be submitted.
- [6] G. Roullet, X. Capet, G. Maze, Global interior eddy available potential energy diagnosed from Argo floats, *Geophysical Research Letters*, 41 (2014) 1651–1656.
- [7] D.J. Ellett, P. Kruseman, G.J. Prangsma, R.T. Pollard, H.M.V. Aken, A. Edwards, H.D. Dooley, W.J. Gould, J.A. Businger, J.G. Harvey, Water Masses and Mesoscale Circulation of North Rockall Trough Waters during JASIN 1978, *Philosophical Transactions of the Royal Society A*, 308 (1983) 231–252.
- [8] D.A. Booth, Eddies in the Rockall Trough, *Oceanologica Acta*, 11,3 (1988) 213–219.
- [9] J.E. Ullgren a, M. White Observations of mesoscale variability in the Rockall Trough, *Deep-Sea Research I*, 64 (2012) 1–8.
- [10] T.J. Sherwin, D. Aleynik, E. Dumont, M.E. Inall, Deep drivers of mesoscale circulation in the central Rockall Trough, *Ocean Science*, 11 (2015) 343–359.
- [11] A.M. Treguier , S. Theeten , E.P. Chassignet, T. Penduff, R. Smith , L. Talley, J.O. Beismann, C. Böning, The North Atlantic Subpolar Gyre in Four High-Resolution Models, *Journal of Physical Oceanography*, 35 (2005) 757–774.
- [12] A. Köhl, Generation and Stability of a Quasi-Permanent Vortex in the Lofoten Basin, *Journal of Physical Oceanography*, 37 (2007) 2637–2651.
- [13] R.P. Raj, L. Chafik, J.E.Ø. Nilsen, T. Eldevik, I. Halo, The Lofoten Vortex of the Nordic Seas, *Deep-Sea Research I*, 96 (2015) 1–14.
- [14] D.L. Volkov, A.A. Kubryakov, R. Lumpkin, Formation and variability of the Lofoten basin vortex in a high-resolution ocean model, *Deep-Sea Research I*, 105 (2015) 142–157.
- [15] A.F. Shchepetkin, J.C. McWilliams, The regional oceanic modeling system (ROMS) : a split-explicit, free-surface, topography-following-coordinate oceanic model, *Ocean Modelling*, 9 (2005) 347–404.
- [16] L. Debreu, P. Marchesiello, P. Penven, G. Cambon, Two-way nesting in split-explicit ocean models : Algorithms, implementation and validation, *Ocean Modelling* 49–50 (2012) 1–21.

- [17] D.B. Chelton, R.A. De Szoeke, M.G. Schlax, Geographical Variability of the First Baroclinic Rossby Radius of Deformation, *Journal of Physical Oceanography*, 28 (1998) 433–460.
- [18] F. Lemarié, J. Kurian, A.F. Shchepetkin, M.J. Molemaker, F. Colas, J.C. McWilliams, Are there inescapable issues prohibiting the use of terrain-following coordinates in climate models ? *Ocean Modelling*, 42 (2012) 57–79.
- [19] L. Umlauf, H. Burchard, A generic length-scale equation for geophysical turbulence models, *Journal of Marine Research*, 61 (2003) 235–265.
- [20] J. Gula, M.J. Molemaker, J.C. McWilliam, Gulf Stream Dynamics along the Southeastern U.S. Seaboard, *Journal of Physical Oceanography*, 45 (2015) 690–715.
- [21] C.W. Hughes, B.A. De Cuevas, Why Western Boundary Currents in Realistic Oceans are Inviscid : A Link between Form Stress and Bottom Pressure Torques, *Journal if Physical Oceanography*, 31 (2001) 2871–2885.
- [22] M.J. Molemaker, J.C. McWilliams, W.K. Dewar, Submesoscale instability and generation of mesoscale anticyclones near a separation of the California Undercurrent, *Journal of Physical Oceanography*, 45 (2015) 613–629.
- [23] J. Gula, M.J. Molemaker, J.C. McWilliams, Topographic generation of submesoscale centrifugal instability and energy dissipation, *Nature Communications*, 7 (2016) 12811
- [24] J. Gula, T.M. Blacic, R.E. Todd, Submesoscale Coherent Vortices in the Gulf Stream, *Geophysical Research Letters*, 46 (2019)
- [25] E. van Sebille, S.M. Griffies, R. Abernathey, T.P. Adams, P. Berloff , A. Biastoch, B. Blanke, E.P. Chassignet, Y. Cheng, C.J. Cotter, E. Deleersnijder, K. Döös, H.F. Drake, S. Drijfhout, S.F. Gary, A.W. Heemink, J. Kjellsson, I.M. Koszalka, M. Lange, C. Lique, G.A. MacGilchrist, R. Marsh, C.G.M. Adame, R. McAdam, F. Nencioli, C.B. Paris, M.D. Piggott, J.A. Polton, S. Rühs, S.H.A.M. Shah, Ma.D. Thomas, J. Wang, P.J. Wolfram, L. Zanna, J.D. Zika, Lagrangian ocean analysis : Fundamentals and practices, *Ocean Modelling*, 121 (2018) 49–75.